

THE FAR-INFRARED BACKGROUND CORRELATION WITH CMB LENSING

YONG-SEON SONG¹, ASANTHA COORAY², LLOYD KNOX¹ AND MATIAS ZALDARRIAGA³

¹ Department of Physics, University of California, Davis, CA 95616, USA
email: yssong@bubba.ucdavis.edu, lknox@ucdavis.edu

² Theoretical Astrophysics, California Institute of Technology, Pasadena, CA 91125, USA
email: asante@caltech.edu

³ Physics Department, New York University, New York, NY 10003, USA
Institute for Advanced Study, Einstein Drive, Princeton NJ 08540, USA
email: mz3@nyu.edu

Submitted to ApJ

ABSTRACT

The intervening large-scale structure distorts cosmic microwave background (CMB) anisotropies via gravitational lensing. The same large-scale structure, traced by dusty star-forming galaxies, also induces anisotropies in the far-infrared background (FIRB). We investigate the resulting inter-dependence of the FIRB and CMB with a halo model for the FIRB. In particular, we calculate the cross-correlation between the lensing potential and the FIRB. The lensing potential can be quadratically estimated from CMB temperature and/or polarization maps. We show that the cross-correlation can be measured with high signal-to-noise with data from the *Planck Surveyor*. We discuss how such a measurement can be used to understand the nature of FIRB sources and their relation to the distribution of dark matter.

Subject headings: cosmology: theory – cosmology: observation – diffuse radiation – infrared:cosmology: weak lensing – cosmology: formation – galaxies: evolution

1. INTRODUCTION

Dusty star-forming galaxies give rise to a far-infrared background (FIRB) (Puget et al. 1996; Fixsen et al. 1998; Dwek et al. 1998; Schlegel Finkbeiner & Davis 1998; Lagache et al. 1999; Guiderdoni et al. 1998; Blain 1999). Correlations in the large-scale structure traced by these contributing sources lead to correlated fluctuations in the FIRB (Bond et al. 1986; Scott & White 1999; Haiman & Knox 2000; hereafter HK00; Knox et al. 2001; Magliocchetti 2001). At arcminute scales and more, fluctuation power associated with the source distribution can potentially be detected with Planck and other planned CMB experiments with channels at frequencies around and above 300 GHz (Knox et al. 2001).

The same large-scale structure that generates FIRB anisotropy also generates anisotropy in the CMB in several ways. These include modifications due to scattering via free electrons in galaxy clusters, such as the thermal Sunyaev-Zel'dovich effect (Sunyaev & Zel'dovich 1980), and modifications imposed by the time evolving gravitational field, such as the integrated Sachs-Wolfe effect (Sachs & Wolfe 1967). The large-scale structure mass field also deflects CMB photons propagating to us from the last scattering surface via the gravitational lensing effect (Seljak 1996). Since the lensing effect on CMB anisotropies is second order in temperature fluctuations, it induces non-Gaussian signatures in the temperature data; the cross-correlation between the lensing effect and other secondary anisotropies, such as SZ or ISW, contributes to the temperature bispectrum (Goldberg & Spergel 1998; Cooray & Hu 2000; Seljak & Zaldarriaga 1999).

We extend previous discussions on correlations between the CMB and large-scale structure and consider the cross-correlation of CMB anisotropies and FIRB fluctuations. The FIRB contributes significantly at the high frequency end of certain CMB experiments, such as the 350 GHz, 545 GHz and 850 GHz channels of the High Frequency In-

strument (HFI) of the Planck Surveyor. Over this range of frequencies, and in regions of the sky with low galactic dust emission, the FIRB stands out as the dominant source of fluctuation power over a wide range of angular scales (Knox et al. 2001). We model the expected cross-correlation between lensing potentials and the FIRB through a physically motivated semi-analytical approach involving the halo model (Scherrer & Bertschinger 1991; Seljak 2000; Scoccimarro et al. 2000; Cooray & Sheth 2002).

Though the lensing potential-FIRB correlation leads to a bispectrum or a three-point correlation function in CMB temperature and FIRB, we suggest a direct cross-correlation between lensing potentials and FIRB. Our suggestion follows from recent discussions in the literature on how to reconstruct lensing potentials associated with CMB lensing, especially through higher order statistics such as quadratic estimates optimized for the lensing extraction in temperature and polarization data (Zaldarriaga & Seljak 1999; Hu 2001b; Hu & Okamoto 2001; Cooray & Kesden 2002). We consider this possibility for planned missions such as Planck.

Using reasonable assumptions, we show that Planck has sufficient sensitivity for a detection of the lensing-FIRB correlation. A detection of such a correlation would allow us to test how well the sources of the FIRB trace the large-scale mass distribution. While semi-analytic approaches such as the halo model suggest a high correlation, the exact correlation as measured will allow us to further refine details of these models and to understand certain physical properties of contributing FIRB sources.

The layout of the paper is as follows. In Section 2 we present the halo model for FIRB fluctuations. In Section 3 we revisit the angular power spectrum of the FIRB and describe the cross correlation between the FIRB and a quadratic function of the CMB temperature map. The quadratic CMB statistic is an estimator for the lensing

potential. In section 4 we discuss associated errors and the extent to which the FIRB-lensing correlation can be detected. We conclude with a discussion of our results in Section 5. We refer the reader to Haiman & Knox (2000; hereafter HK00) and Knox et al. (2001) for initial details on our calculation of correlations in the FIRB. More details of the halo approach to large-scale structure are available in the recent review by Cooray & Sheth (2002). For a review of our observational knowledge of the FIRB see Hauser & Dwek (2001). While we provide a general derivation of the FIRB-lensing correlation, when illustrating our results we assume a Λ CDM cosmological model with $\Omega_m = 0.35, \Omega_\Lambda = 0.65, \Omega_b = 0.05, h = 0.65$. To describe linear clustering, we use the transfer function given by Eisenstein & Hu (1999) and normalize fluctuations to COBE (Bunn & White 1997) such that $\sigma_8 = 0.86$.

2. HALO APPROACH TO THE FIRB

As in HK00, we write the FIRB Rayleigh–Jeans temperature ($T_{\text{RJ}} \equiv I_\nu / (2k_B)(c/\nu)^2$) at frequency ν and in direction \hat{n} as a sum of the mean and the fluctuation about the mean

$$\begin{aligned} T_{\text{RJ}}(\hat{n}, \nu) &= \bar{T}_{\text{RJ}}(\nu) + \delta T_{\text{RJ}}(\hat{n}, \nu) \\ &= \frac{c^2}{2k_B \nu^2} \int dr a(r) \bar{j}(\nu, r) \left[1 + \frac{\delta j(r\hat{n}, \nu, r)}{j(\nu, r)} \right]. \end{aligned} \quad (1)$$

Here, r is the radial distance from us to a redshift of z and $\bar{j}(\nu, z)$ is the mean emissivity of the dust. Note that we have related the excess fluctuation in FIRB temperature to a fluctuation in the emissivity, $\delta j(r\hat{n}, \nu, z)$.

We adopt the HK00 model for the mean emissivity as a function of redshift and frequency. The key ingredients of this model are the history of ultra-violet radiation and dust production. Both of these are assumed to be proportional to a star-formation rate, which here and in the HK00 fiducial model we take to be that of Madau (1997). By further assuming the optical properties of the dust (Draine & Lee 1984) we then derive the comoving mean emissivity, $\bar{j}_\nu(z)$. The dust and UV production proportionality constants are chosen so that the resulting FIRB agrees with inferences from *COBE*/FIRAS data (Fixsen et al. 1998).

To model fluctuations of the FIRB, we assume that the sources of this emissivity are galaxies so that $\delta j(r\hat{n}, \nu, z) / \bar{j}(\nu, z) = \delta_{\text{gal}}$ where $n_{\text{gal}} = \bar{n}_{\text{gal}}(1 + \delta_{\text{gal}})$. Our modeling differs from that in HK00 in that we calculate the statistical relation of the galaxy number density field to the dark matter by making assumptions about how these galaxies populate dark matter halos; i.e., we use the ‘halo approach’ to large-scale structure.

The halo approach to large-scale structure involves a simplified description of the complex distribution of dark matter as consisting of a population of dark matter halos. The spatial distribution of any tracer field of the large-scale structure, such as galaxies, is described through the relation of the tracer field to that of the dark matter halo distribution. The halo approach has now been widely discussed in the literature to understand the clustering of dark matter, galaxies and baryons (Scherrer & Bertschinger 1991; Scoccimarro et al. 2000; Cooray & Sheth 2002). The necessary inputs for the halo-based calculations come from either analytical tools, such as the

dark matter halo mass function, or from numerical simulations, such as the distribution of dark matter within each halo.

The two-point correlation function of the object of interest in a halo model has two terms; the first is a two-point correlation function within each dark matter halo and the second is the two-point correlation function between points which are in different halos. The halo distribution is taken to trace the linear fluctuations with biases which are predictable from analytical arguments. The time evolution of the correlation function is naturally determined by this semi-analytic model since clustering evolution can be related to the evolution of the halo mass function and any evolution of physical properties related to halos. As we find below, the halo model has the advantage that one does not need to specify a priori quantities such as the bias and evolution of fields that trace the mass distribution of the large-scale structure.

Following Scherrer & Bertschinger (1991) and Scoccimarro et al. (2000) we can write the two-point function of the mass distribution as

$$\begin{aligned} \bar{\rho} \xi(\mathbf{x} - \mathbf{x}', z) &= \\ &= \int n(m, z) m^2 dm \int d^3 y u_m(\mathbf{y}, z) u_m(\mathbf{y} + \mathbf{x} - \mathbf{x}', z) \\ &+ \int n(m_1, z) m_1 dm_1 \int n(m_2, z) m_2 dm_2 \int d^3 x_1 u_{m_1}(\mathbf{x} - \mathbf{x}_1, z) \\ &\times \int d^3 x_2 u_{m_2}(\mathbf{x}' - \mathbf{x}_2, z) \xi(\mathbf{x}_1 - \mathbf{x}_2; m_1, m_2, z), \end{aligned} \quad (2)$$

where we have written out explicitly the redshift-dependence of the correlation function; hereafter, for simplicity, we usually drop this redshift-dependence when writing our expressions. In above, $n(m)$ is the mass function describing the number density of collapsed objects with given mass m :

$$\frac{m^2 n(m)}{\bar{\rho}} \frac{dm}{m} = \nu f(\nu) \frac{d\nu}{\nu} \quad (3)$$

where $\bar{\rho}$ is the background density and $f(\nu)$ is defined, following arguments given by Press & Schechter (PS; 1974) as

$$\nu f(\nu) = \frac{1}{2} \left(\frac{\nu}{2\pi} \right)^{1/2} \exp\left(-\frac{\nu}{2}\right). \quad (4)$$

Here, ν is given by

$$\nu \equiv \frac{\delta_{\text{sc}}^2(z)}{\sigma^2(m, z)}, \quad (5)$$

where $\delta_{\text{sc}}^2(z)$ is the critical density for spherical clustering and $\sigma^2(m, z)$ is the density fluctuation smoothed with a tophat filter at a redshift of z corresponding to mass scale of m . Useful fitting formula for $\delta_{\text{sc}}(z)$ and related variables can be found in Henry (2000). The first term of equation (1) is the two-point correlation function within one halo, the second term is the two-point correlation function between points being in two different halos and $u_m(\mathbf{x})$ represents mass distribution in the collapsed region.

We apply the NFW (Navarro Frenk & White 1997) profile for the mass distribution in the collapsed region with

$$u_m(r) = \frac{\rho_s}{(r/r_s)(1+r/r_s)^2}, \quad (6)$$

where r_s is the core radius and ρ_s is the density at r_s . We can also get r_s from the known mean concentration

relation, $\bar{c} = r_{vir}/r_s$. We calculate the virial radius of each halo following spherical collapse arguments such that $M = 4\pi r_v^3 \Delta(z) \rho_b / 3$, where $\Delta(z)$ is the overdensity of collapse and ρ_b is the background matter density today. We use comoving coordinates throughout.

The mean concentration parameter \bar{c} is given by (Bullock et al. 2001; Jing 2000)

$$\bar{c} = \frac{9}{1+z} \left[\frac{m}{m_*(z)} \right]^{-0.13} \quad (7)$$

where $m_*(z)$ is the critical mass at given z . The density profile in Fourier space is

$$u(k|m) = \int_0^{r_{vir}} dr 4\pi r^2 \frac{\sin kr}{kr} \frac{\rho(r|m)}{m}, \quad (8)$$

where r_{vir} is the virialized radius of the collapsed object.

The Fourier transformation of equation (1) gives the power spectrum

$$\begin{aligned} P_{dm}(k) &= P_{dm}^{1h}(k) + P_{dm}^{2h}(k) \\ P_{dm}^{1h}(k) &= \int dm n(m) \left(\frac{m}{\bar{\rho}} \right)^2 u(k|m)^2 \\ P_{dm}^{2h}(k) &= \int dm_1 n(m_1) \frac{m_1}{\bar{\rho}} u(k|m_1) \\ &\quad \times \int dm_2 n(m_2) \frac{m_2}{\bar{\rho}} u(k|m_2) \\ &\quad \times P_{hh}(k|m_1, m_2). \end{aligned} \quad (9)$$

Here, $P_{hh}(k|m_1, m_2)$ is the halo-halo power spectrum which we take to be related to the power spectrum of the linear density field, $P_{dm}^L(k)$ by

$$P_{hh}(k|m_1, m_2) = b_1(m_1)b_1(m_2)P_{dm}^L(k). \quad (10)$$

The halo biasing b_1 is (Mo et al. 1997)

$$b_1(m) = 1 + \frac{\nu - 1}{\delta_{sc}(z_1)}. \quad (11)$$

We assume that the dust giving rise to the FIRB is all in galaxies. To describe clustering properties of these dusty galaxies, we modify the halo model for dark matter to describe point sources following previous discussions in the literature (Seljak 2000; Jing et al. 1998).

An important ingredient is how these galaxies occupy dark matter halos. Following Scoccimarro et al. (2000); Cooray & Sheth (2002), we model this halo occupation number, the average number of galaxies in each dark matter halo of mass m , through a simple relation of the form

$$\langle N_{gal}(m) \rangle = A_{gal} (m/m_0)^{p_{gal}}. \quad (12)$$

When illustrating our results, we will take $A_{gal} = 0.7$, $m_0 = 4.2 \times 10^{12}$ and $p_{gal} = 0.8$ consistent with what is suggested in the literature for the halo occupation number of blue, star-forming, galaxies (Scoccimarro et al. 2000; Cooray & Sheth 2002). Besides these parameters, we also set a lower bound on the halo mass, at $m_c = 10^{11} M_\odot/h$, in which dusty galaxies may exist. This accounts for the fact that baryons may not collapse and cool to form stars in low mass halos as well as to account for the fact that star-formation may not be efficient due to processes such as supernova winds which may expel any remaining gas in such small mass halos (Benson et al. 2001; Kauffmann et al. 1993).

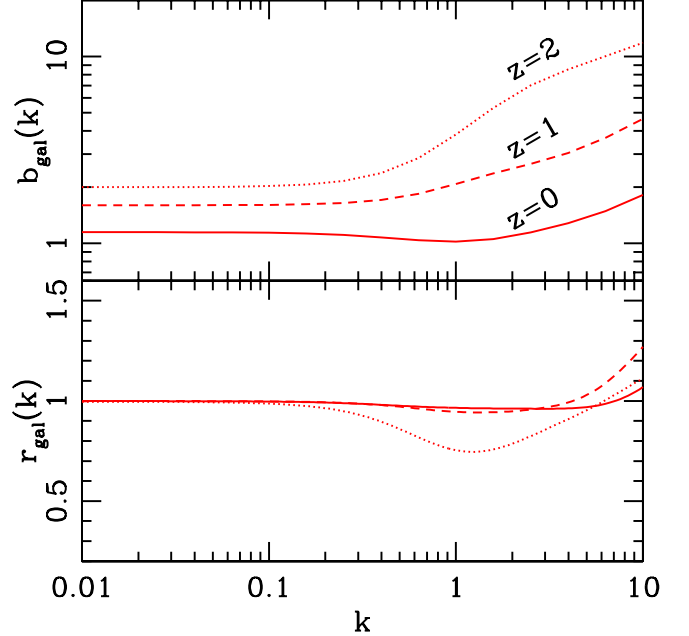


FIG. 1.— Galaxy bias as a function of k for our fiducial halo model at $z = 0, 1, 2$ (upper panel) and galaxy–dark matter density contrast correlation coefficient (lower panel).

Note that we have described the halo occupation number of sources that contribute to FIRB with a description that is consistent for blue galaxies at low redshifts. While these late-type galaxies are expected to trace dusty-starbursts that form the FIRB, our choice of parameters is also consistent with another consideration. The non-linear clustering of sources in the IRAS Point Source Redshift Survey Catalog (PSCz), based on 60 μm fluxes, is well produced by a halo occupation number consistent with the above set of parameters for p , A_{gal} , and m_0 (Scoccimarro et al. 2000; Cooray 2002). These sources are also likely to trace the dusty-starbursts that contribute to FIRB. An additional complication, which we return to later, is if FIRB sources are associated with either mergers or active galactic nuclei.

To describe galaxy clustering at the two-point level we also need the second moment, $\langle N_{gal}(N_{gal}-1) \rangle$ of the galaxy halo occupation distribution. Given our limited knowledge, we take the simplest approach involving a Poisson distribution such that $\langle N_{gal}(N_{gal}-1) \rangle = \langle N_{gal}(m) \rangle^2$. This assumption is consistent with numerical simulations especially at the high mass end while at the low mass end of the mass function, when $\langle N_{gal}(m) \rangle < 1$, evidence exists for departures from a Poisson distribution (Scoccimarro et al. 2000; Cooray & Sheth 2002).

With information related to the halo occupation number, we can write the power spectrum of dusty galaxies, again with two terms:

$$\begin{aligned} P_{gal}(k) &= P_{gal}^{1h}(k) + P_{gal}^{2h}(k) \\ P_{gal}^{1h}(k) &= \int dm n(m) \left(\frac{\langle N_{gal}(m) \rangle}{\bar{n}_{gal}(m)} \right)^2 u(k|m)^p \\ P_{gal}^{2h}(k) &= \int dm_1 n(m_1) \frac{\langle N_{gal}(m_1) \rangle}{\bar{n}_{gal}(m_1)} u(k|m_1) \end{aligned}$$

$$\begin{aligned} & \times \int dm_2 n(m_2) \frac{\langle N_{\text{gal}}(m_2) \rangle}{\bar{n}_{\text{gal}}(m_2)} u(k|m_2) \\ & \times P_{hh}(k|m_1, m_2). \end{aligned} \quad (13)$$

Here, p accounts for the possibility that at least one galaxy may reside in the center of each halo. Thus, we set $p = 1$ when $\langle N_{\text{gal}} \rangle < 1$ and otherwise $p = 2$. Here, \bar{n}_{gal} is the mean density of FIRB sources given by

$$\bar{n}_{\text{gal}} = \int dm n(m) \langle N_{\text{gal}}(m) \rangle. \quad (14)$$

The angular power spectrum of FIRB fluctuations can now be obtained by projecting the three-dimensional dusty galaxy power spectrum along the line of sight following standard techniques such as the Limber approximation. The cross-correlation between lensing and the FIRB, however, depends on the correlation of dusty galaxy and dark matter distributions. The halo model provides a simple calculation of this cross-correlation and we write

$$\begin{aligned} P_{dm-gal}(k) &= P_{dm-gal}^{1h}(k) + P_{dm-gal}^{2h}(k) \\ P_{dm-gal}^{1h}(k) &= \int dm n(m) \frac{m}{\bar{\rho}} \frac{\langle N_{\text{gal}}(m) \rangle}{\bar{n}_{\text{gal}}(m)} u(k|m)^p \\ P_{dm-gal}^{2h}(k) &= \int dm_1 n(m_1) \frac{m_1}{\bar{\rho}} u(k|m_1) \\ & \times \int dm_2 n(m_2) \frac{\langle N_{\text{gal}}(m_2) \rangle}{\bar{n}_{\text{gal}}(m_2)} u(k|m_2) \\ & \times P_{hh}(k|m_1, m_2). \end{aligned} \quad (15)$$

The halo approach can be used to estimate the dusty galaxy bias, b_{gal} , and correlation, r_{gal} , both as a function of scale, k , and redshift z . We define these two quantities as

$$\begin{aligned} b_{\text{gal}}(k, z) &= \sqrt{\frac{P_{\text{gal}}(k, z)}{P_{\text{dm}}(k, z)}} \\ r_{\text{gal}}(k, z) &= \frac{P_{dm-gal}}{\sqrt{P_{\text{gal}} P_{\text{dm}}}}, \end{aligned} \quad (16)$$

and plot them in Fig.1 as a function of k for three redshifts ($z = 0, 1$ and 2). Note that $b_{\text{gal}}(k)$ is constant at the large spatial scales corresponding to the linear regime. This large-scale bias, under the halo model, is simply

$$b_{\text{gal}}(k) = \int dm n(m) b_1(m) \frac{\langle N_{\text{gal}}(m) \rangle}{\bar{n}}. \quad (17)$$

At non-linear scales bias increases due to the choice of $p = 1$ when $\langle N_{\text{gal}} \rangle < 1$. The behavior of $r_{\text{gal}}(k)$ can also be understood from the halo model. At linear scales, galaxies trace the dark matter such that they perfectly correlate with each other. At non-linear scales, $r_{\text{gal}}(k)$ is greater than unity since the galaxy power spectrum is defined such that, following the standard definitions, it does not include the shot-noise part associated with the finite number of galaxies (Seljak 2000).

3. ANGULAR POWER SPECTRA

In this paper we are interested in measuring the cross-correlation between FIRB fluctuations and the lensing effect on CMB anisotropies. For the purpose of this discussion, we will describe lensing through the associated projected potential, ϕ , along the line of sight

$$\phi(\hat{\mathbf{n}}) = -2 \int dr \frac{d_A(r_0 - r)}{d_A(r) d_A(r_0)} \Phi(r, \hat{\mathbf{m}}r), \quad (18)$$

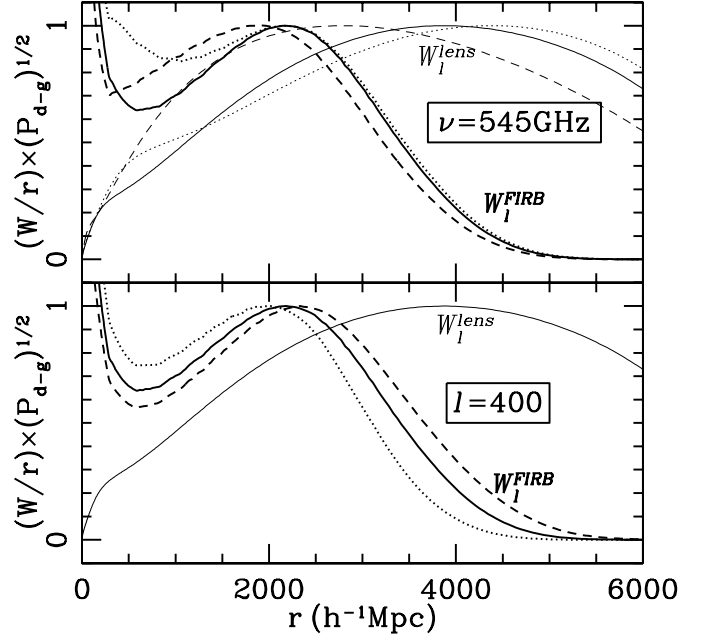


FIG. 2.— Integrand of equation (27). Here we plot the integrand of equation (27) broken up into two factors, $W^{len}(k, \nu, z)/r\sqrt{P_{dm-gal}(l/r)}$ (light) and $W^F(k, \nu, z)/r\sqrt{P_{dm-gal}(l/r)}$ (heavy). Top panel shows $l = 100$ (dashed), $l = 400$ (solid) and $l = 1000$ (dotted) at $\nu = 545$ GHz and bottom panel shows $\nu = 353$ GHz (dashed), $\nu = 545$ GHz (solid) and $\nu = 852$ GHz (dotted) at $l = 400$.

where $r_0 \equiv r(z = 1100)$ corresponds to the radial distance to background CMB fluctuations which act as a source for lensing and Φ is the gravitational potential field. Here, d_A is the comoving angular diameter distance and, in a spatially-flat cosmology, $d_A \rightarrow r$. Note that the deflection angle of a CMB photon is given by the gradient of this projected potential, $\alpha(\hat{\mathbf{n}}) = \nabla\phi(\hat{\mathbf{n}})$.

First, we will consider the three power spectra associated with the projected lensing potential, FIRB fluctuations at frequency ν , F_ν , and the cross-correlation between the two. We use flat-sky coordinates throughout the paper and write the Fourier transform of quantities as

$$X(\mathbf{l}) = \int d^2\theta X(\theta) e^{-i\mathbf{l}\cdot\theta}, \quad (19)$$

where $X \equiv F, \phi$ for FIRB and lensing potentials respectively. We define power spectra of these quantities and the cross-power spectrum such that

$$\langle F_\nu(\mathbf{l}) F_\nu(\mathbf{l}') \rangle = (2\pi)^2 \delta_D(\mathbf{l} + \mathbf{l}') C_l^{FF}(\nu), \quad (20)$$

$$\langle \phi(\mathbf{l}) \phi(\mathbf{l}') \rangle = (2\pi)^2 \delta_D(\mathbf{l} + \mathbf{l}') C_l^{\phi\phi}, \quad (21)$$

$$\langle F_\nu(\mathbf{l}) \phi(\mathbf{l}') \rangle = (2\pi)^2 \delta_D(\mathbf{l} + \mathbf{l}') C_l^{F\phi}(\nu). \quad (22)$$

$$(23)$$

We can write Fourier coefficients for fluctuations in either the FIRB or lensing potential as

$$X(\mathbf{l}) = \int \frac{d^3k}{(2\pi)^3} \int d^2\theta \int dr W^X(k, r) \delta_X(\vec{k}, r) e^{-i(\mathbf{l}-\mathbf{k}r)\cdot\theta}. \quad (24)$$

Following Knox et al. (2001), we write the FIRB weighting function at a given frequency ν as

$$\begin{aligned} W^F(z; \nu) &\equiv a(z) \bar{j}(\nu, z) / (2k_B)(c/\nu)^2 \text{ and} \\ \delta_F &= \delta_{\text{gal}}. \end{aligned} \quad (25)$$

Similarly, for lensing potentials,

$$W^\phi(k, z) \equiv -3 \frac{\Omega_m}{a(r)} \left(\frac{H_0}{k} \right)^2 \frac{d_A(r_0 - r)}{d_A(r) d_A(r_0)} \text{ and} \\ \delta_\phi = \delta_{\text{dm}}. \quad (26)$$

We have used Poisson's equation to replace the potential field with the dark matter density field, resulting in the k -dependence of the window function.

As written in equations (25) and (26), and discussed earlier, FIRB fluctuations trace that of contributing galaxies, while lensing traces fluctuations in the dark matter field. For illustration purposes, we plot both FIRB and lensing weight functions in Fig. 2 as a function of multipole, or angular scale, and frequency. Note that the lensing weight function, while peaking at nearly half the angular diameter distance to background source, is a broad function in redshift space. This allows lensing potentials to be correlated with a wide variety of large-scale structure tracer fields. The main result from this comparison is that the lensing and FIRB weight functions overlap with each other over a wide range in radial distance space. As we find later, this substantial overlap results in a significant correlation between lensing potentials and FIRB fluctuations.

Using the weighting functions in radial space, we can now calculate the angular power spectra of FIRB and lensing potential fluctuations as well as the cross angular power spectrum between the FIRB and lensing potentials. We make use of the Limber approximation (Limber 1954; Kaiser 1992) and write

$$C_l^{\phi\phi} = \int \frac{dr}{d_A^2} [W^{\text{len}}(k, z)]^2 P_{\text{dm}} \left[k = \frac{l}{d_A}, z \right], \\ C_l^{\text{FF}}(\nu) = \int \frac{dr}{d_A^2} [W^F(z; \nu)]^2 P_{\text{gal}} \left[k = \frac{l}{d_A}, z \right], \\ C_l^{\text{F}\phi}(\nu) = \int \frac{dr}{d_A^2} W^F(z; \nu) W^{\text{len}}(k, z) P_{\text{dm-gal}} \left[k = \frac{l}{d_A}, z \right], \quad (27)$$

for lensing-lensing, FIRB-FIRB and FIRB-lensing power spectra.

In Fig. 3 we show the angular power spectrum of the FIRB for our fiducial model at 545 GHz. Here, we have calculated five predictions for the FIRB signal including two constant bias models that trace the non-linear dark matter power spectrum under the formulation given by Peacock & Dodds (1996) with bias equal to 1 (lower curve) and 3 (upper curve). The solid curve in the middle is the prediction for the FIRB with our halo model. Because $\nu = 545$ GHz is much greater than the frequency of peak intensity for a 2.73 K black body, the CMB signal is significantly smaller than the FIRB signal.

For comparison, in Fig. 3, we show the two contributions to the FIRB power spectrum under the halo model involving 1- and 2-halo terms. As shown, the FIRB clustering at tens of arcminute scales and above is described by correlations of FIRB sources in different halos while at arcminute scales, the 1-halo term due to correlations of sources within the same halo dominates. At these small scales, however, instrumental noise starts to contribute rapidly contaminating the FIRB clustering at smallest scales.

In Fig. 4, we show the cross-correlation between FIRB fluctuations at 545 GHz and the lensing potential. The

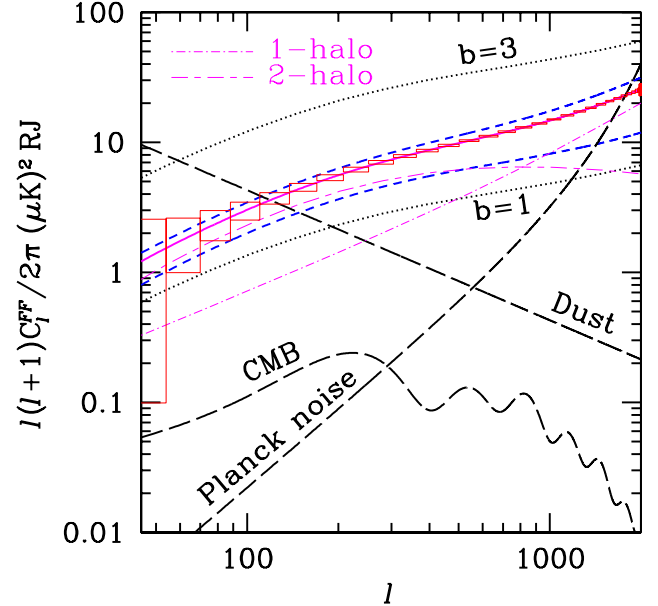


FIG. 3.— Angular power spectra at 545 GHz of our fiducial FIRB model (solid with error boxes), CMB (dot-dash), galactic dust averaged over cleanest 10% of the sky (short/long dash) and Planck noise (dashed). The curves labeled 1-h and 2-h show the 1- and 2-halo contributions to the FIRB power spectrum. Error boxes are for measurement of FIRB power spectrum by Planck using only the cleanest 10% of the sky and including the contributions from unsubtracted galactic dust. The dashed lines below the fiducial FIRB model are for angular power spectra for FIRB models with $m_c \rightarrow 10^{10} M_\odot/h$ (lower) and $p_{\text{gal}} \rightarrow 0.9$ (upper). Dotted lines are constant-bias FIRB models with $b = 1$ (lower) and $b = 3$ (upper).

curves shown here follow those of Fig. 3. As shown, cross-correlation in the multipole range of interest is dominated by the 2-halo term. This captures the large scale linear correlations between FIRB sources and dark matter in different halos instead of the clustering of FIRB sources and dark matter in the same halo. This dependence on the two-halo term is understandable from the weight functions plotted in Fig. 1. As shown there, the cross-correlation peaks where the weight functions overlap the most and this is at radial distance corresponding to redshifts of 1 and higher. At such distances, the non-linearities, captured by the 1-halo term, do not dominate.

The strength of the correlation between ϕ and F is quantified by the cross-correlation coefficient

$$r_{\text{corr}}(l) = \frac{C_l^{\text{F}\phi}}{\sqrt{C_l^{\phi\phi} C_l^{\text{FF}}}}. \quad (28)$$

In Fig. 5 we show that the correlation is moderate, as expected from the rough similarity of the weighting functions. Note that if fraction $1 - \epsilon$ of the FIRB signal is *completely* dependent on the lensing signal (i.e., can be predicted from it) then we expect $1 - r_{\text{corr}} \simeq 0.5\epsilon^2$. A significant uncorrelated component still results in a r_{corr} near unity; e.g., $\epsilon = 0.4 \rightarrow r_{\text{corr}} = 0.92$.

In addition to cross-correlation, we can also define a bias factor in Fourier space relating FIRB fluctuations and dark

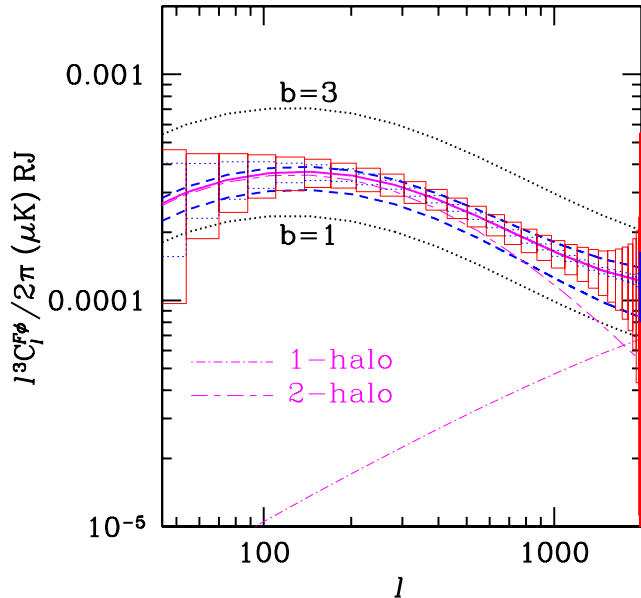


FIG. 4.— Angular power spectrum of FIRB–CMB lensing cross–correlation function at 545 GHz for same FIRB models as in Fig. 3. The curves labeled 1-h and 2-h show the 1- and 2-halo contributions to the cross power spectrum. Note that in the range of angular scales of interest to *Planck*, all contributions effectively come from the 2-halo term or the large scale correlations between FIRB sources and dark matter between different halos. Error boxes assume use of 10% of the sky, include the contributions from unsubtracted dust and *do not* include polarization information. Solid (dashed) error boxes are for *Planck* (no) noise.

matter traced by lensing potentials, such that

$$b(l) = \sqrt{\frac{C_l^{\text{FF}}}{C_l^{\phi\phi}}}. \quad (29)$$

We also plot this bias factor and its associated errors on the bottom panel of Fig. 5.

4. ERROR FORECASTS

Here we consider expected measurement errors on the various signals predicted in the previous sections and shown in Figures 3, 4, and 5. First, we consider the expected errors on the detection of lensing potential power spectrum and the FIRB power spectrum. Then we will discuss the associated errors on the determination of the cross-correlation between FIRB and lensing.

4.1. Lensing

In the case of lensing power spectrum, we assume that the deflection angle associated with the CMB lensing can be constructed from quadratic statistics involving temperature fluctuations (Hu & Okamoto 2001; Cooray & Kesden 2002).

To understand the mechanism involved, first notice that lensing involves a remapping of the CMB temperature (Seljak 1996; Zaldarriaga 2000; Hu & Okamoto 2001; Cooray & Kesden 2002) such that

$$\begin{aligned} \tilde{\Theta}(\hat{\mathbf{n}}) &= \Theta[\hat{\mathbf{n}} + \nabla\phi(\hat{\mathbf{n}})] \\ &= \Theta(\hat{\mathbf{n}}) + \nabla_i\phi(\hat{\mathbf{n}})\nabla^i\Theta(\hat{\mathbf{n}}) \\ &\quad + \frac{1}{2}\nabla_i\phi(\hat{\mathbf{n}})\nabla_j\phi(\hat{\mathbf{n}})\nabla^i\nabla^j\Theta(\hat{\mathbf{n}}) + \dots \end{aligned} \quad (30)$$

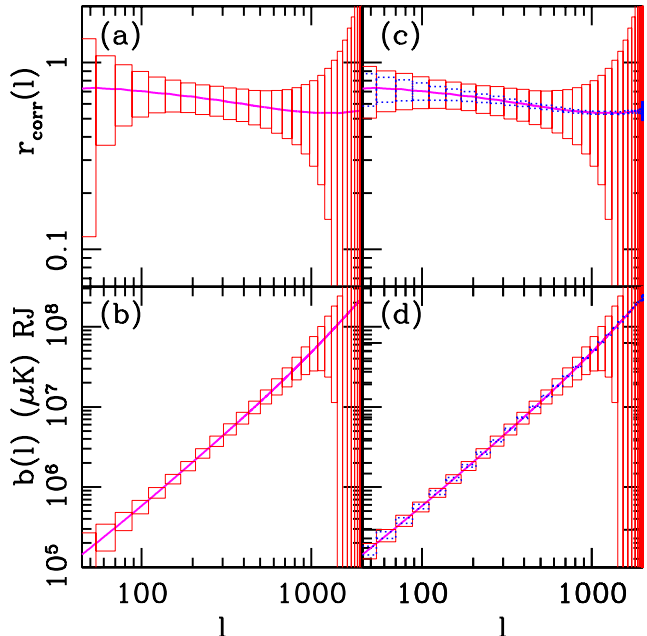


FIG. 5.— *Top*: The correlation coefficient (see equation (28)) at 545 GHz. (a) Error boxes assume the observation of the cleanest 10% of the sky with *Planck* noise and include the contributions from unsubtracted dust. (c) For comparison in this panel we show the error boxes obtained when there is no dust contribution to the FIRB map (solid line) and, in addition, no noise contribution to the lensing reconstruction such that $N_l^{\phi\phi} = 0$ (dashed line). *Bottom*: The bias coefficient for FIRB fluctuations relative to that of the lensing potential field. The error boxes follow those in the top panel.

where $\Theta(\hat{\mathbf{n}})$ is the unlensed primary component of CMB, the contribution at the last scattering surface, and $\tilde{\Theta}(\hat{\mathbf{n}})$ is the total contribution observed today after modifications due to gravitational lensing deflections during the transit. To extract information related to lensing potentials, now consider a simple quadratic statistic involving the squared temperature map, which in Fourier space can be written as

$$\hat{\Theta}^2(\mathbf{l}) = \int \frac{d^2\mathbf{l}_1}{(2\pi)^2} W(\mathbf{l}, \mathbf{l}_1) \tilde{\Theta}(\mathbf{l}_1) \tilde{\Theta}(\mathbf{l} - \mathbf{l}_1), \quad (31)$$

where W is a filter that acts on the CMB temperature and can be derived by the requirement that an ensemble average of this quadratic statistic returns an estimator for ϕ , $\langle \hat{\Theta}^2(\mathbf{l}) \rangle \equiv \hat{\phi}(\mathbf{l})$, with a minimum noise contribution. Taking the Fourier transform of equation (30), and substituting for $\tilde{\Theta}(\mathbf{l})$ in equation (31), one can obtain the required filter as

$$W(\mathbf{l}, \mathbf{l}_1) = N_l^{\phi\phi} \frac{[\mathbf{l} \cdot \mathbf{l}_1 C_{l_1}^{\Theta} + \mathbf{l} \cdot (\mathbf{l} - \mathbf{l}_1) C_{|\mathbf{l} - \mathbf{l}_1|}^{\Theta}]}{2C_{l_1}^{\text{tot}} C_{|\mathbf{l} - \mathbf{l}_1|}^{\text{tot}}}, \quad (32)$$

with a normalization given by

$$[N_l^{\phi\phi}]^{-1} = \int \frac{d^2\mathbf{l}_1}{(2\pi)^2} \frac{[\mathbf{l} \cdot \mathbf{l}_1 C_{l_1}^{\Theta} + \mathbf{l} \cdot (\mathbf{l} - \mathbf{l}_1) C_{|\mathbf{l} - \mathbf{l}_1|}^{\Theta}]^2}{2C_{l_1}^{\text{tot}} C_{|\mathbf{l} - \mathbf{l}_1|}^{\text{tot}}}. \quad (33)$$

Here, C_l^{Θ} is the power spectrum of unlensed primordial temperature fluctuations, as measured at the last scattering surface, while C_l^{tot} accounts for all contributions to the temperature power spectrum such that $C_l^{\text{tot}} = C_l^{\text{lensed-CMB}} + C_l^{\text{noise}} + C_l^{\text{fore}}$. Here, $C_l^{\text{lensed-CMB}}$ is the

CMB power spectrum after gravitational lensing, C_l^{noise} is detector and instrumental noise contributions, and C_l^{fore} describes the contribution due to any foregrounds and secondary effects, such as the SZ effect.

Note that the variance of the filtered quadratic temperature map,

$$\langle \hat{\Theta}^2(\mathbf{l}) \hat{\Theta}^2(\mathbf{l}') \rangle = (2\pi)^2 \delta_D(\mathbf{l} + \mathbf{l}') \left[C_l^{\phi\phi} + N_l^{\phi\phi} \right], \quad (34)$$

returns the lensing potential power spectrum plus an associated Gaussian noise bias given by $N_l^{\phi\phi}$. We note that even in the case of a CMB experiment with no detector noise, the reconstructed potential, under the quadratic statistic technique described above, is biased as $N_l^{\phi\phi}$ has contributions from primordial CMB fluctuations. This implies that the correlation coefficient defined in equation (28) is not the correlation coefficient one measures between the FIRB map and the reconstructed ϕ map, as described above, even for an ideal experiment. This noise bias, however, can be eliminated possibly through a different reconstruction technique involving an unbiased estimator of the lensing deflection potential. In order to generalize our discussion, we ignore this noise-bias and treat $N_l^{\phi\phi}$ as the error contribution associated with the reconstructed $C_l^{\phi\phi}$. Thus, correlation coefficients we plot in Fig. 5 are those that one would measure by correlating the FIRB map with an unbiased estimator of the deflection angle.

In addition to the case with temperature we have just discussed, the polarization field can also be used to reconstruct ϕ (Guzik, Seljak, & Zaldarriaga 2000; Benabed et al. 2000; Hu & Okamoto 2001; Cooray & Kesden 2002), though we perform no error forecasts for polarization data here.

When estimating $N_l^{\phi\phi}$, we consider two experiments corresponding to Planck and a no-detector noise, cosmic variance limited, experiment. In the case of Planck, we use tabulated values for its detector sensitivities and resolutions, or beam sizes, following Cooray et al. (2000) to calculate C_l^{noise} . In the case of the cosmic variance limited experiment, we set $C_l^{\text{noise}} = 0$ and take a maximum l of 3000. to which we integrate equation (33). In both these experimental possibilities, we set $C_l^{\text{fore}} = 0$.

4.2. FIRB

On the FIRB side, we expect a significant contribution to the angular power spectrum at 545 GHz from galactic dust. The level of the dust power spectrum shown in Fig. 3 is for that in the cleanest 10% of $5^\circ \times 5^\circ$ patches (Knox et al. 2001). The average level in the cleanest 50% is about 10 times higher.

We approximate the effect of dust contamination by including it as an unsubtracted noise source with a power spectrum given by C_l^{D} . The error on the FIRB-FIRB power spectrum is

$$\Delta C_l^{\text{FF}} = \frac{1}{\sqrt{(2l+1)f_{\text{sky}}}} C_l^{\text{FF,tot}}, \quad (35)$$

where following Knox et al. (2001)

$$C_l^{\text{FF,tot}} = (C_l^{\text{FF}} + C_l^{\text{D}} + N_l^{\text{FF}}) \quad \text{and} \quad N_l^{\text{FF}} \equiv \Delta_{T_{\text{RJ}}}^2 e^{l(l+1)\sigma^2/8\ln 2}. \quad (36)$$

Here, N_l^{FF} is due to instrumental noise in the beam-deconvolved maps. For example, the *Planck* 545 GHz channel has $\sigma = 5.0'$ and (on average) $\Delta_{T_{\text{RJ}}} = 13\mu\text{K} - \text{arcmin}$. Throughout we use the $\nu = 545$ GHz channel as our probe of the FIRB though valuable, and complementary, information does lie in other channels at both higher and lower frequencies.

Equation (35) is formally correct for a single-frequency measurement if the power spectrum of the dust is perfectly known and the dust is a statistically isotropic Gaussian random field. These conditions do not hold; this equation only serves as a rough guide, with dust increasing the errors when $C_l^{\text{D}} \gtrsim C_l^{\text{FF}}$ and having little effect when $C_l^{\text{D}} \ll C_l^{\text{FF}}$. Throughout we restrict our forecasting to results from the cleanest 10% of the sky, using the appropriate dust level.

4.3. Lensing-FIRB

Following our discussion on lensing reconstruction, one can use the estimator for the deflection angle, or the projected potential, to measure the cross-correlation with FIRB fluctuations. Thus, similar to equation (34), we can write $\langle \hat{\Theta}^2(\mathbf{l}) F(\mathbf{l}') \rangle = (2\pi)^2 \delta_D(\mathbf{l} + \mathbf{l}') C_l^{\text{F}\phi}$ as an estimate of the cross-power spectrum between lensing potentials and FIRB fluctuations. In Fig. 4 we plot $C_l^{\text{F}\phi}$. Note that while $C_l^{\phi\phi}$ is biased under quadratic temperature reconstruction techniques, the cross-correlation power spectrum between lensing potential and FIRB is unbiased; this is due to the fact that FIRB fluctuations are assumed to be uncorrelated with unlensed temperature anisotropies $\langle \Theta(\mathbf{l}) F(\mathbf{l}') \rangle = 0$.

Following our discussion of errors on lensing and FIRB fluctuation power spectra, we can write the expected error on $C_l^{\text{F}\phi}$ as

$$\Delta C_l^{\text{F}\phi} = \sqrt{\frac{1}{(2l+1)f_{\text{sky}}}} \left[\left(C_l^{\text{F}\phi} \right)^2 + (C_l^{\phi\phi,\text{tot}})(C_l^{\text{FF,tot}}) \right]^{1/2}, \quad (37)$$

where $C_l^{\phi\phi,\text{tot}} = C_l^{\phi\phi} + N_l^{\phi\phi}$ is the total contribution in the ϕ power spectrum.

The associated error on the correlation coefficient and the bias factor can be calculated by propagating errors related to $C_l^{\phi\phi}$, C_l^{FF} , and, $C_l^{\text{F}\phi}$. For reference, we reproduce the final result for these errors here. In the case of $r_{\text{corr}}(l) \left(\equiv C_l^{\text{F}\phi} / \sqrt{C_l^{\phi\phi} C_l^{\text{FF}}} \right)$:

$$(\Delta r)^2 = \sum_l r_{\text{corr}}^2(l) \left\{ \left(\frac{\Delta C_l^{\text{F}\phi}}{C_l^{\text{F}\phi}} \right)^2 + \frac{1}{2(2l+1)f_{\text{sky}}} \times \left[\left(\frac{C_l^{\phi\phi,\text{tot}}}{C_l^{\phi\phi}} + \frac{C_l^{\text{FF,tot}}}{C_l^{\text{FF}}} \right) \left(\frac{C_l^{\phi\phi,\text{tot}}}{C_l^{\phi\phi}} + \frac{C_l^{\text{FF,tot}}}{C_l^{\text{FF}}} - 4C_l^{\text{F}\phi} \right) \right] \right\}, \quad (38)$$

while, in the case of $b(l) \left(\equiv \sqrt{C_l^{\text{FF}}/C_l^{\phi\phi}} \right)$:

$$(\Delta b)^2 = \sum_l \frac{b^2(l)}{2(2l+1)f_{\text{sky}}} \left(\frac{C_l^{\phi\phi,\text{tot}}}{C_l^{\phi\phi}} - \frac{C_l^{\text{FF,tot}}}{C_l^{\text{FF}}} \right)^2. \quad (39)$$

5. DISCUSSION

We now discuss the main results of our paper. We have introduced a semi-analytic approach to describe the FIRB fluctuations. The model involves a distribution of dark matter halos populated by dusty, starforming galaxies. The basic ingredients of the calculation include properties of this dark matter distribution, such as the mass function and clustering properties of dark matter halos, and properties of the sources responsible for the FIRB. To describe these sources we have introduced a relation, the halo occupation number, that attempts to capture how FIRB sources populate dark matter halos. This model can be used to calculate measurable properties of the sources such as their bias as a function of redshift and their spatial correlation with the underlying dark matter as a function of redshift.

The approach presented here differs from previous attempts to model the fluctuations in the FIRB. HK00 used several biasing models, all of which were scale-independent. The one most similar to our calculation here assumed all the FIRB sources were in $10^{12} M_{\odot}$ halos and used the biasing prescription of Mo & White (1996). Because we include a range of halo masses extending below $10^{12} M_{\odot}$ and because we take the FIRB mean to be $\sqrt{2}$ lower than HK00 did our power spectra have smaller amplitudes. The fluctuation power we predict is also smaller than that in Knox et al. (2001) who used a constant $b = 3$ amplification of the non-linear power spectrum calculated using the fitting formula of Peacock & Dodds (1996).

Even though we predict a smaller power spectrum than in the constant bias models we still expect FIRB fluctuations to be detectable in upcoming high frequency experiments such as Planck. Any multifrequency detection will allow the testing of our models and hopefully the extraction of interesting properties of our universe such as the evolution of the star-formation rate. We do not discuss such possibilities in detail here as they have been already addressed in Knox et al. (2001) and references therein.

In this paper we have gone beyond the FIRB fluctuation power and focused on the cross-correlation between FIRB sources and the dark matter as traced by the intervening lensing potential that deflected CMB photons propagating to us. Note that previous studies have already suggested that experiments such as Planck will detect the lensing potential power spectrum with considerable signal-to-noise ratios (Zaldarriaga & Seljak 1999; Zaldarriaga 2000; Hu & Okamoto 2001; Cooray & Kesden 2002). In addition to the separate detections of FIRB and projected lensing potential power we have suggested that one can also perform a combined study to measure the cross-correlation between FIRB fluctuations and the lensing potential.

We have discussed an extension of the estimators suggested for lensing reconstruction in CMB data. Using quadratic statistics one can define an estimator of the deflection angle, which can then be directly correlated with a high frequency map where FIRB fluctuations are expected to dominate. Such a direct approach avoids complications associated with other methods for extracting the lensing-FIRB cross power spectrum such as the direct measure of the three point function. As discussed in the literature, the FIRB-lensing correlation leads to a three-point correlation function, or a bispectrum in Fourier space (Goldberg

& Spergel 1998; Cooray & Hu 2000). Note that measuring the full configuration dependence of this bispectrum is difficult and currently limited by computational methods and measurement techniques. While improvements are expected, our suggested technique avoids these issues by combing the different three point function configurations in a particular way.

As shown in Fig. 4, we find a considerable correlation between FIRB fluctuations and the lensing potential. As illustrated in Fig. 2, this is due to the broad overlap between the respective radial weighting functions. Such a high correlation coefficient also leads to the conclusion that upcoming CMB experiments will be able to detect the cross power spectrum between FIRB and lensing with high signal-to-noise. For Planck, we expect the cumulative signal-to-noise to be of order 40 in the $\nu = 545$ GHz channel.

The high signal to noise expected for the detection of the cross correlation and of the FIRB and lensing power spectra suggests that we will be able to test our underlying model for the clustering of FIRB sources. As we discussed our approach needed two main ingredients, the bias of FIRB contributing sources which was calculated in the halo model, and the star formation rate which is needed to obtain FIRB weighting function. In turn, the halo approach depends on how starforming dusty galaxies populate dark matter halos. As shown in Fig. 3 and Fig. 4 we expect that different values of the model parameters can be distinguished with the level of noise expected for Planck.

In Fig. 5, we summarize our results with respect to how well the projected correlation coefficient, $r_{\text{corr}}(l)$, and the bias factor, $b(l)$, can be measured with upcoming Planck data. While Planck allows a reliable detection of the correlation coefficient as well as bias out to a multipole of ~ 1000 , there are further improvements one can hope to achieve in the post-Planck era. As summarized in Fig. 5(c), in the case of the correlation coefficient, the error is dominated by the uncertainty associated with the lensing reconstruction. With improved data involving better angular resolution and noise one can hope to reach the limiting case of a perfect experiment which we have demonstrated with a dashed line Fig. 5(c).

A few words of caution are required at this point. Note that we have described the FIRB and its fluctuations as coming only from dusty starburst galaxies. In addition to the stellar contribution, there is also some from dust associated with torii surrounding active galactic nuclei. While the fraction of AGN contribution at far-infrared wavelengths could be as high as 30% to 40% (Almaini et al. 2001; Risaliti et al. 2002), we have limited information on their redshift evolution so we have not included them in our calculation. The inclusion of AGNs within the halo model is trivial, the problems arise when trying to calculate the weighting function.

Another caveat comes from our simple description of how submm sources populate halos. While we have described them through a halo occupation number, the physics is likely to be more complicated especially if dusty star formation is associated with mergers. With a merger rate proportional to $N_{\text{gal}}^2(m)$, the effective occupation number will probably depend on a higher power of mass

than considered here. In such a scenario, we expect source bias to be larger with an increase in clustering power compared to the results presented here. Such an increase should be detectable and constrained using observational data.

While these issues may complicate the direct interpretation of the observations, a reliable detection of the FIRB-lensing correlation can allow one to introduce more sophisticated analysis techniques to try to understand these complicating factors. For example, the two power spectra and the cross-power spectrum can be combined and written as $C_l^{FF} = b(l)C_l^{\phi\phi}$ and $C_l^{F\phi} = b(l)r(l)C_l^{\phi\phi}$, which can be inverted with appropriate techniques to obtain $r(k, z)$ and $b(k, z)$. Such an inversion requires accurate information on the FIRB radial weight function which can be obtained observationally through the redshift distribution of sources that contribute to FIRB. While unresolved surveys such as Planck will not allow such studies, in the future, targeted studies of resolved FIRB sources, over small but representative patches of sky may provide the necessary information. Constraints on this emissivity as a function of redshift from current data are discussed in Gispert et al. (2000), Chary & Elbaz (2001) and Takeuchi et al. (2001). With an inversion of two-dimensional clustering to three-dimensions one can eventually constrain various aspects of the halo model such as the occupation number (Cooray 2002). While previous studies have motivated the use of FIRB fluctuations alone to understand an important aspect of the large scale structure and its evolution history, we also suggest that cross-clustering aspects, such as between FIRB and dark matter as traced by gravitational lensing of CMB also plays an important role.

We thank Z. Haiman for the use of emissivity functions, $\hat{j}(\nu, z)$, that he calculated. AC is supported at Caltech by a senior research fellowship from the Sherman Fairchild foundation and DOE. LK is supported by NASA Grant NAG5-11098. MZ is supported by NSF grants AST 0098606 and PHY 0116590, and by the David and Lucille Packard Foundation Fellowship for Science and Engineering. This research was supported in part by the NSF under Grant No. PHY99-07949.

REFERENCES

- Almaini, O., Scott, S. E., Dunlop, J. S. et al. 2001, MNRAS submitted, astro-ph/0108400
 Benabed, K., Bernardeau, F., van Waerbeke, L. 2001, PRD, 63, 043501.
 Benson, A. J., Frenck, C. S., Baugh, C. M., Cole, S., Lacey, C. G. 2001, MNRAS, 327, 1041
 Blain, A.W., Jameson, A., Smail, I., Longair, M.S., Kneib, J.-P., & Ivison, R.J. 1999, MNRAS 309, 715
 Bond, J. R., Carr, B. & Hogan, C. 1986, ApJ 306, 428
 Bullock, J. S., Dekel, A. & Kolatt, T. S. 2001, MNRAS, 321, 559
 Bunn, E. F. & White, M. 1997, ApJ, 480, 6
 Chary, R. & Elbaz, D. 2001, ApJ 556, 562
 Cooray, A. 2001, PRD, 64, 043516
 Cooray, A. & Hu, W. 2000, ApJ, 534, 533
 Cooray, A., Hu, W. & Termark, M. 2000, ApJ, 540, 1.
 Cooray, A. & Kesden, M. 2002, PRD submitted, astro-ph/0204068
 Cooray, A. & Sheth, R. 2002, Physics Reports in press, astro-ph/0206508.
 Cooray, A. 2002, ApJL, 576, 10.
 Draine, B. T., & Lee, H. M. 1984, ApJ, 285, 89
 Dwek, A. et al. 1998, ApJ, 508, 106
 Eisenstein, D. & Hu, W. 1999, ApJ, 511, 5
 Fixsen, D. J., et al. 1998, ApJ, 508, 123
 Gispert, R., Lagache, G. & Puget, J.L. 2000, A&A 360, 1
 Goldberg, D. M. & Spergel, D. N. 1998, PRD, 59, 103002
 Guiderdoni, B., Hivon, E., Bouchet, F.R. & Maffei, B. 1998, MNRAS, 295, 877
 Guzik, J., Seljak, U. ; & Zaldarriaga, M. 2000, PRD, 62, 43517
 Haiman, Z., & Knox, L. 2000, ApJ, 534, 11(HK00)
 Hauser, M.G. & Dwek, E., ARA&A 39, 249
 Henry, J. P. 2000, ApJ, 534, 565.
 Hu, W. 2001a, PRD, 64, 083005
 Hu, W. 2001b, PRD, 65, 023003
 Hu, W. & Okamoto, T. 2002, ApJ, 574, 566.
 Jing, Y. P. 2000, ApJ, 535, 30
 Jing, Y. P., Mo, H. J. & Boerner, G. 1998, ApJ, 494, 1.
 Kaiser, N., 1992, ApJ, 388, 272.
 Kauffmann, G., Colberg, J. M., Diaferio, A., White, S. D. M. 1999, MNRAS, 303, 188
 Knox, L., Cooray, A., Eisenstein, D. & Haiman, Z. 2001, ApJ, 550, 7
 Lagache, G., et al. 1999, A&A, 344, 322
 Limber, D. 1954, ApJ, 119, 655
 Madau, P. 1997, in AIP Conf. Ser. 393, Seventh Astrophys. Conf., Star Formation Near and Far, ed. S. S. Holt & L. G. Mundy (New York:AIP), 481
 Magliocchetti, M., Moscardine, L., Panuzzo, P., Granato, G.L., De Zotti, G. & Danese, L. 2001, MNRAS 325, 1553
 Mo, H.J., & White, S.D.M. 1996, MNRAS 282, 347
 Mo, H. J., Jing, Y. P., White, S. D. M. 1997, MNRAS, 284, 189
 Navarro, J. F., Frenk, C. S. & White, C. S. 1997, ApJ, 490, 493
 Okamoto, T. & Hu, W. 2002, PRD submitted, astro-ph/0206155
 Peacock, J.A. & Dodds, S.J. 1996, MNRAS, 280, L19
 Press, W. H., Schechter, P. 1974, ApJ, 381, 349
 Puget, J. L., et al. 1996, A&A, 308, L5
 Risaliti, G., elvis, M. & Gilli, R. ApJ 566L 67
 Sachs, R. K. & Wolfe, A. M. 1967, ApJ, 147, 73
 Scherrer, R. J. & Bertschinger, E. 1991, ApJ, 381, 349
 Schlegel, D. J., Finkbeiner, D. P. & Davis, M. 1998, ApJ, 500, 525
 Scoccimarro, R., Sheth, R. K., Hui, L & Jain, B. 2000, ApJ, 546, 20
 Scott, D. & White, M. 1996, A&A 346, 1
 Seljak, U. 1996, ApJ, 463, 1
 Seljak, U. 2000, MNRAS, 318, 203
 Seljak, U. & Zaldarriaga, M. 1999, PRD. 60, 043504.
 Sunyaev, R. A. & Zel'dovich, Y. B. 1980, MNRAS, 190, 413
 Takeuchi et al. 2001, PASJ 53, 37
 Zaldarriaga, M. & Seljak, U. 1999, PRD, 59, 123507.
 Zaldarriaga, M. 2000, PRD, 62, 063510